Transfection of functional proteins with DNA-protein nanogels-lipids complex

Marina Mariconti, Virginie Escriou, Mathieu Morel, Damien Baigl, Céline Hoffmann, Sergii Rudiuk

Transfection of functional proteins with DNA-protein nanogels-lipids complex

Marina Mariconti[1‡], Virginie Escriou[2]*, Mathieu Morel[1], Damien Baigl[1], Céline Hoffmann[2] and Sergii Rudiuk[1]*

[1]*PASTEUR, UMR8640, Department of Chemistry, PSL University, Sorbonne Université, CNRS, Ecole Normale Supérieure, Paris 75005, France*

[2]*Université Paris Cité, CNRS, INSERM, UTCBS, F-75006 Paris, France*

*To whom correspondence may be addressed. Email: sergii.rudiuk@ens.psl.eu or virginie.escriou@u-paris.fr

‡ Current address: ClinSearch, Malakoff, France

Significance

Transfection through cell membrane of a large number of functional proteins embedded into DNA nanogels is investigated. The nanogels of multibiotinylated DNA were loaded with around 100 protein molecules through streptavidin-biotin binding and rendered transfectable by electrostatic complexation with lipidic vectors. This approach was successfully used for transfection of an enzyme, alkaline phosphatase, whose intracellular catalytic activity was observed to strongly increase after transfection. Based on streptavidin-biotin interactions, this biocompatible nanoplatform can be functionalized by both streptavidin- and biotin-tagged proteins, making it a near universal modular system potentially functionalizable with a large number of biological and chemical entities.

Abstract

Using functional proteins for therapeutic purposes due to their high selectivity and/or catalytic properties can enable the control of various cellular processes, however, the transport of active proteins inside living cells remains a major challenge. In contrast, intracellular delivery of nucleic acids has become a routine method for a number of applications in gene therapy, genome-editing or immunization. Here we report a functionalizable platform constituting of DNA-protein nanogel carriers crosslinked through streptavidin-biotin interactions and demonstrate its applicability for intracellular delivery of active proteins. We demonstrate that the nanogels can be loaded with proteins bearing either biotin or streptavidin tags, and can be transfected into living cells after complexation with cationic lipid vectors. In particular we use this approach for transfection of alkaline phosphatase enzyme which is shown to keep its catalytic activity after internalization by mouse melanoma B16 cells, as demonstrated by DDAO-phosphate assay. The resulting functionalized nanogels have dimensions of the order of 100 nm, contain around 100 enzyme molecules and are shown to be transfectable at low lipid concentrations (charge ratio R+/- = 0.75). Low lipid concentrations requested for transfection of the 3-dimensional DNA nanogels ensure low toxicity of our system, which in combination with high local enzyme concentration (~ 100 μM) underlines potential interest of this nanoplatform for biomedical applications.

Introduction

Due to their highly specific biological activities and intrinsic biocompatibility, delivery of active proteins into cells represents great interest not only for fundamental research (1) and intracellular sensing (2), but also for numerous therapeutic applications. (3–5) However, despite their high potential, proteins suffer from chemical and thermal degradation, kidney clearance, and difficulty to penetrate through biological membranes. (6) In particular, enzymes present a major limitation to be sensitive to both medium and the temperature, leading to the loss of their catalytic activity in inappropriate conditions thus limiting their applicability in both enzyme replacement therapy (7, 8) and enzyme prodrug therapy (9, 10). Another aspect requiring consideration is the localization of proteins. Indeed, while most therapeutic proteins currently on the market have an extracellular localization, the intracellular transport of active proteins aiming cytosolic targets could strongly expand their exploitation for biomedical purposes. (11, 12) Yet the transport to the cytosol is still a major challenge, mainly due to physical impediment of the cell membrane and possible protein inactivation due to endocytosis. (13–15)

Various vectorization systems have thus been proposed for protein protection and transfection, such as PEGylation, conjugation with cell-penetrating (CPP) or specifically engineered peptides, and formulations with liposomes or polymeric nanoparticles. (5, 16–18) DNA represents another promising protein carrier in nanomedicine (19, 20), due to its intrinsic biocompatibility, programmability and transfectability. In fact, nucleic acids can be readily transfected into cells by using various non-viral cationic transfection agents, among which, cationic lipids represent the most involved vectors in clinical studies. (21) In this view, recently DNA has been bound to β-galactosidase and glucose oxidase in order to both protect and deliver them into the cells by using lipofectamine as transfection agent. (2, 22) In this case individual enzyme molecules were covalently conjugated to several single-stranded DNA oligonucleotides. In another example, three luciferase molecules inside tubular DNA origami nanostructures were delivered into the cells via polyethylenimine transfection vector. (23) A modular protein delivery system was recently proposed by Ryu et al., where 3 different proteins could be bound to 3 extremities of Y-shape DNA nanostructure via DNA-binding zinc-finger protein tags. (24) This system was successfully applied for cytosolic delivery of therapeutic endogenous tumor suppressor PTEN (phosphatase and tension homolog).

In order to expand DNA-based protein delivery to strong local concentrations of transfected protein, here we propose to incorporate a large number of active protein molecules into three-dimensional DNA nanogel network. We have recently reported a new type of DNA nanogels where the intramolecular crosslinking was achieved not by hybridization or covalent DNA crosslinking, but by noncovalent specific interactions between a multibiotinylated DNA (bt-DNA) and streptavidin. (25, 26) Here, we show two different strategies for functionalization of these nanogels with two model cargo proteins: green fluorescent protein GFP, and alkaline phosphatase (ALP) - enzyme which has been proposed for replacement therapy against this hypophosphatasia disorder (27). And we investigate the possibility of transfection of the resulting functionalized nanogels, containing up to 100 μM local protein concentration, through cell membrane by using lipidic DNA transfection agents.

Results

Formation of complexes between DNA-protein nanogels and cationic vesicles - lipoproplexes

Experimental procedure for preparation, vectorization and transfection of DNA-streptavidin nanogels (NGs) is schematically shown in Figure 1A. The scaffold of the NGs constituted of multibiotinylated 3480 bp DNA (bt-DNA) was prepared by PCR as previously described. (26) Crosslinking of the resulting bt-DNA was performed by adding streptavidin labeled with AlexaFluor633 fluorophore to give fluorescent NGs (NG-633) enabling their tracking and analysis by fluorescence microscopy. The resulting NGs had 114 ± 36 nm apparent diameter, as measured by Atomic Force Microscopy (Figure S1B). For vectorization of the NGs, cationic liposomes constituted of equimolar amounts of zwitterionic lipid DOPE (1,2-dioleoyl-sn-glycero-3-phosphoethanolamine) and the cationic lipid DMAPAP (2-3-[bis-(3-amino-propyl)-amino]-propylamino-N-ditetradecyl carbamoyl methyl-acetamide) were used. (28) In analogy with the formation of DNA-lipid complexes (lipoplexes), in our case the complexation of DNA-protein nanogel with lipids will give complexes which we named lipoproplexes (LPX). We thus investigated the interaction between NG-633 and DMAPAP/DOPE liposomes containing 5% of fluorescent DOPE labeled with fluorescein (FITC). First the colloidal stability was assessed for the LPX-633 obtained at different charge ratios (R+/-) by fluorescence microscopy (Figure S2). We considered the charge of the nanogels to be dependent only on the DNA component, as streptavidin was shown not to affect the zeta-potential of bt-DNA upon its folding into nanogels, (26) and the charge concentration of the liposomes was calculated by considering the DMAPAP to have 3 positive groups at physiological pH. It was found that aggregation of the LPX occurred at R+/- higher than 1.5. We thus fixed the ratio R+/- = 1.5 and analyzed the resulting LPX by flow cytometry, a method which enables co-detection of different fluorophores within individual particles of nanometric size (29). The resulting dot-plots for NGs-633 only, FITC-labeled liposomes only and LPX-633 are given in the Figure 1B. For NGs and liposomes the dot plots demonstrate only AlexaFluor633 and FITC signals respectively. However, when NGs and liposomes were mixed together, a large population of particles containing both fluorophores was detected. The observation that the mean FITC fluorescence in the complexes decreased can be explained by FRET energy transfer between the fluorophores, which further confirms electrostatic binding between DNA-protein nanogels and cationic lipids leading to the formation of the lipoproplexes.

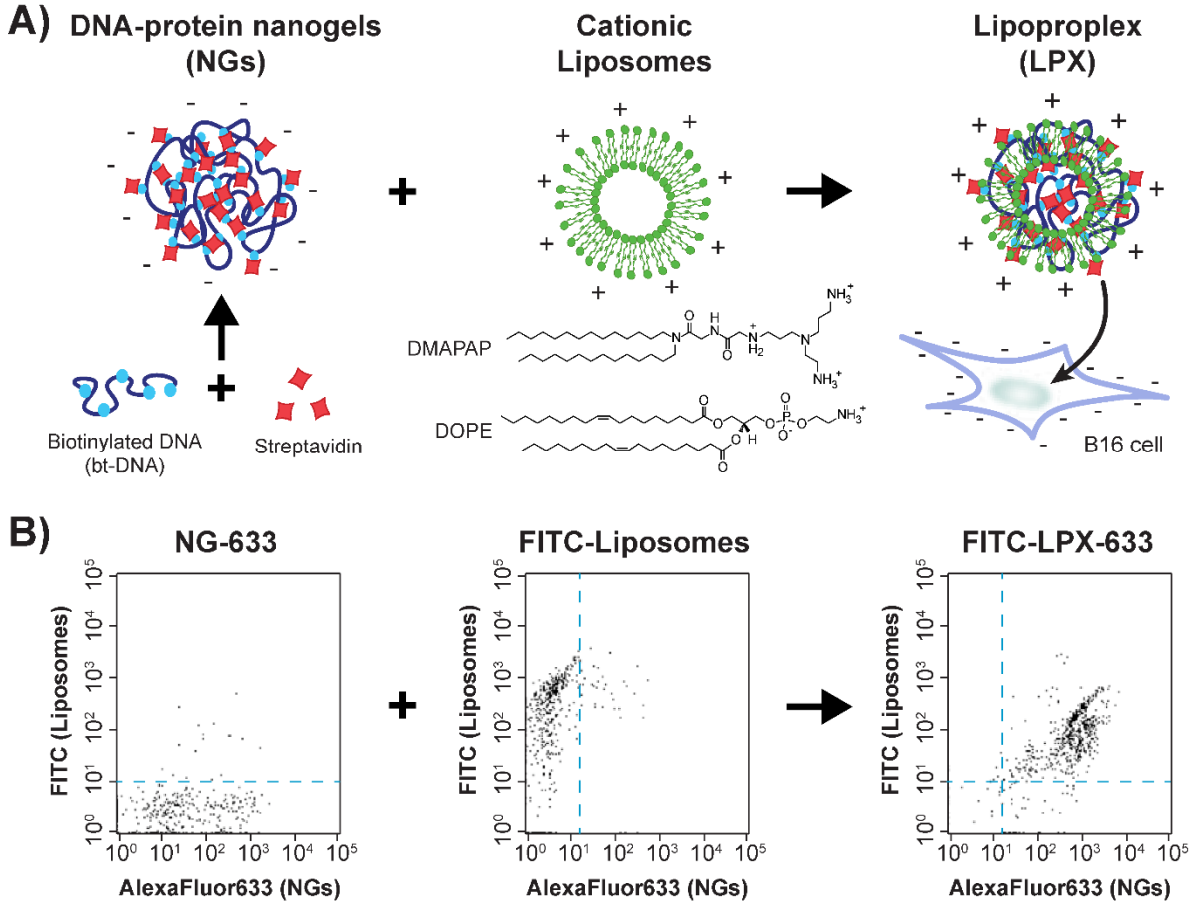

Figure 1. Preparation and characterization of lipoproplexes. A) Scheme of lipoproplex preparation by electrostatic binding of DNA-protein nanogels with cationic liposomes, and their consequent transfection into B16 cells. B) Flow cytometry analysis of DNA nanogels labeled with AlexaFluor633 (NG-633, left), liposomes labeled with FITC (middle) and the resulting lipoproplex complex of the fluorescent nanogels with fluorescent liposomes (FITC-LPX-633, right). The dot-plots represents the fluorescence intensity of the liposomes (FITC: λ_{Ex} = 488 nm; λ_{Em} = 525/30 nm) versus the fluorescence intensity of the NGs (AlexaFluor633, λ_{Ex} = 640 nm; λ_{Em} = 661/19 nm). Blue dotted lines demonstrate a threshold determined thanks to non-fluorescent particles for each population. [NG-633] = 2 µM (in DNA charge); [liposomes] = 3 µM (in DMAPAP charge). All measurements are performed in 10 mM phosphate buffer pH 7.4, [NaCl] = 75 mM.

Transfection of lipoproplexes into cells

The possibility of transfection of the NGs-633 into living cells by their vectorization with cationic liposomes was then investigated with B16 mice melanoma cells. Lipoproplexes (or control solution containing NGs-633 in absence of liposomes) were incubated on the sub-confluent cells in presence of DMEM medium without serum for 2 hours (Figure 2A). Cells were then fixed and stained for subsequent microscopy observations. No NGs were observed within the cells in the control sample after treating them with NGs in absence of liposomes (Figure 2B, left). In contrast, when the cells were treated with NGs complexed with liposomes, fluorescent signal of AlexaFluor633 was clearly observed as red spots within the cells. By performing confocal microscopy acquisition at different *Z*-planes, the presence of the NGs-633 in the same focal planes as cytoskeleton and nucleus was confirmed thus proving that the NGs could be internalized by the cells (Figure 2B right). Liposomes were thus necessary to transfect the nanogels inside the cells. These observations were also confirmed by widefield fluorescence microscopy observations (Figure

S3), where all tested lipoproplexes demonstrated corresponding fluorescence inside B16 cells, regardless of the fluorescent labeling. In contrast, only poor fluorescent signal was detected in B16 cells in the control samples where cells were treated with NG-633 in absence of liposomes or with free AlexaFluor633-streptavidin protein (not incorporated into the NGs) in presence of liposomes. Contrary to several previous reports (30–32) on transfection of DNA-based nanomaterials, we did not detect any internalization of our nanogels in cells in absence of the transfection agent. This difference in internalization could be due to a difference in rigidity between the highly structured tetrahedral DNA nanostructures having edges and corners (31) and our soft nanogels, as it has been demonstrated that the penetration through the membrane depends on the rigidity of the particle (33). On the other hand, it has already been shown that the use of a transfection agent could increase the internalization of a DNA-based nanogel in cells (32). Moreover, we propose that this agent can allow the nanogel to escape degradation in lysosomes. Indeed, Liang et al. showed that bare DNA tetrahedron, after endocytosis, ends up trapped in lysosomes (31), whereas transfection agents, such as cationic lipids, are known to allow the exit of the endosome.

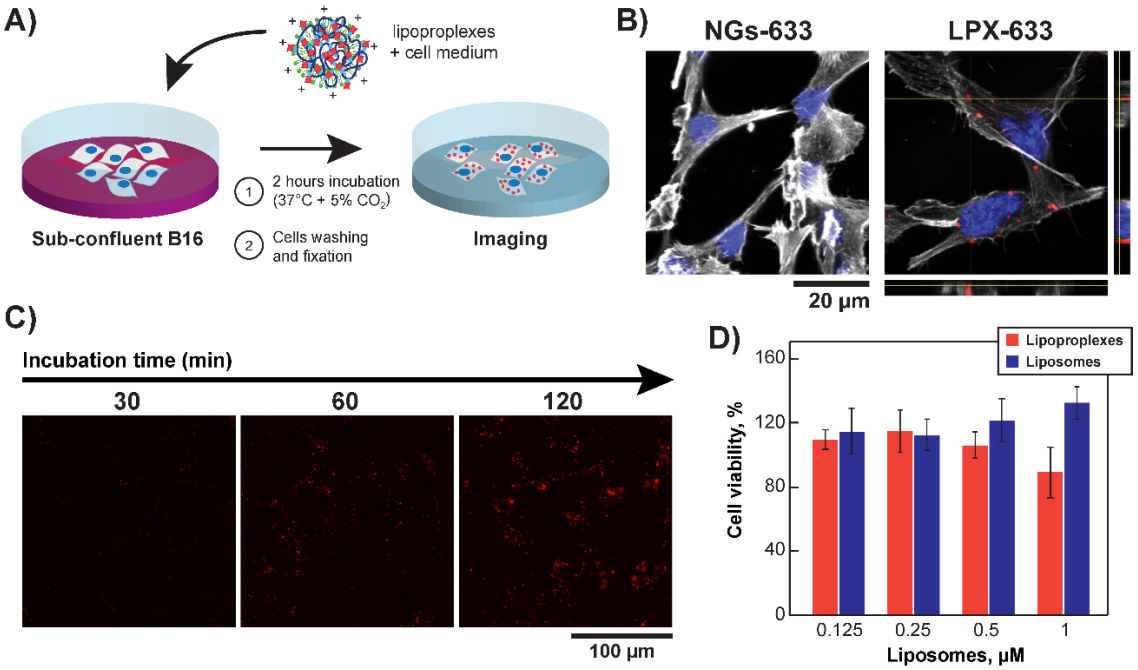

Figure 2. Internalization of DNA-protein nanogels mediated by cationic liposomes. A) Schematic representation of lipoproplex transfection experimental procedure. B) Confocal microscopy observation of B16 cells treated with AlexaFluor633-labeled nanogels in absence (NG-633) and in presence (LPX-633) of transfection lipids after 2h of incubation. Grey color corresponds to actin labeled with phalloidin (λ_{Ex}= 488 nm and λ_{Em} = 495-550 nm), blue to the nucleus stained with DAPI (λ_{Ex}= 405 nm and λ_{Em} = 415-450 nm), and red to nanogels containing AlexaFluor633-labeled streptavidin (λ_{Ex}= 638 nm and λ_{Em} = 645-700 nm). Orthogonal views are given for the cells transfected with LPX-633. C) Widefield fluorescence microscopy images of B16 cells transfected with Alexafluor633-labeled lipoproplexes at different incubation times (λ_{Ex}= 578 ± 11 nm and λ_{Em} = 641 ± 38 nm). D) MTT cell viability assay for B16 cells transfected with different concentrations of lipoproplexes analyzed 26 hours post-transfection. Cell viability is expressed in percentage compared to untreated cells.

The kinetics of lipoproplex internalization for up to 2 hours of transfection was analyzed. Lipoproplex samples (or controls corresponding to NGs in absence of liposomes) were incubated with cells for 30, 60 or 120 minutes, before cell fixation and widefield fluorescence imaging (Figures 2C and S4). We observed that nanogel internalization

progressively increased upon incubation (Figure S5). The toxicity of the lipoproplexes after internalization in B16 cells was then assessed with MTT assay (Figure 2D). (34) It was unaffected (~100% of viable cells) at low and intermediate concentrations of transfected lipoproplexes and only slightly decreased to 90% at the highest tested lipoproplex concentration. At all used concentrations, the cationic liposomes alone were not toxic for the B16 cells. The detection by confocal microscopy of the nanogels inside the cells 24 hours after transfection (Figure S6), further confirmed their biocompatibility and stability in the cellular microenvironment.

Transfection of GFP-loaded lipoproplexes

We then explored the possibility of loading biotinylated cargo proteins into already formed NGs. Biotinylated green fluorescent protein (bt-GFP) was used as model protein due to its fluorescent properties. The preparation of GFP-loaded nanogels (GFP-NGs) was conducted in two steps: i) DNA-protein nanogels were formed with AlexaFluor633-functionalized streptavidin in the conditions described above (Figure S1B), and ii) bt-GFPs was added and bound to remaining available streptavidin sites on the nanogels (Figure 3A). Resulting NGs were first characterized by flow cytometry (Figures 3B and S7A). Colocalization of the GFP with AlexaFluor633 fluorescence in the NGs demonstrates successful formation of GFP-functionalized NGs (GFP-NGs-633). By AFM we observed the increase of the mean apparent diameter of the nanogels from 114 ± 36 nm to 130 ± 51 nm upon treatment with bt-GFP (Figure S1C), which was also attributed to the presence of the loaded GFP. These NGs were then complexed with non-fluorescent cationic liposomes in order to form the functionalized lipoproplexes GFP-LPX-633. Flow cytometry (Figure S7B) demonstrated that the formation of the lipoproplexes did not interfere with GFP functionality, since the signal of functional GFP protein was still co-detected with AlexaFluor633 from the nanogels after adding the liposomes. B16 cells were then transfected with these GFP-LPX-633 and observed by confocal microscopy. Figure 3C shows the presence of fluorescent GFP colocalized with nanogels within the cells only when the nanogels have been complexed with the liposomes. Biotinylated GFP protein has thus been successfully transfected into the cells within DNA-streptavidin nanogels complexed with cationic liposome vector.

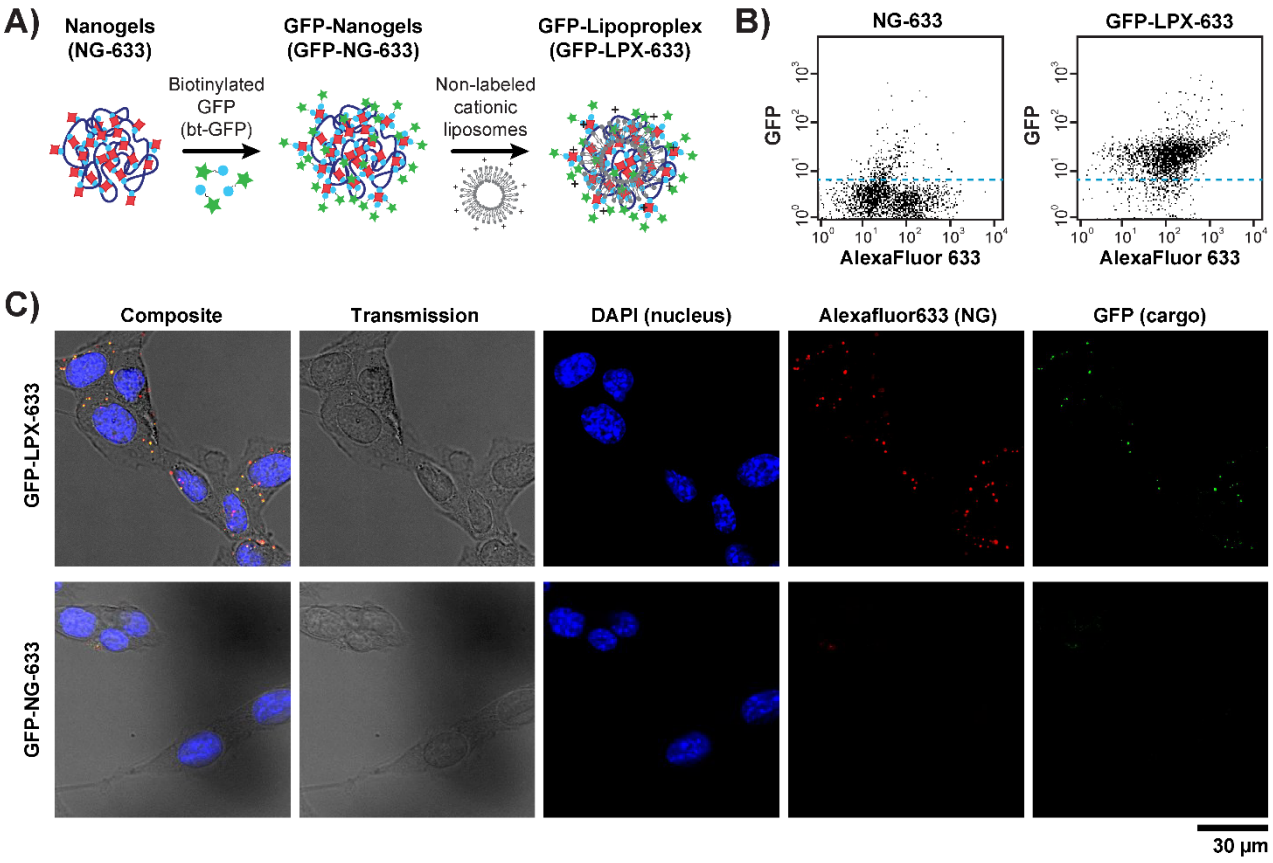

Figure 3. Transfection of lipoproplexes functionalized with GFP. A) Scheme of post-functionalization of NG-633 with biotinylated GFP (bt-GFP) and preparation of the corresponding lipoproplexes (GFP-LPX-633). B) Flow cytometry dot plots for NG-633 (left) and GFP-LPX-633 (right). Blue dotted lines show a threshold for each population. C) Transmission and confocal microscopy images of B16 cells incubated either with GFP-NG-633 (bottom) or with GFP-LPX-633 (top). Cells are imaged in transmission light and overlayed with fluorescence signal from confocal observations. Green color corresponds to GFP cargo protein (λ_{Ex}= 488 nm and λ_{Em} = 495-550 nm), blue to the nucleus stained with DAPI (λ_{Ex}= 405 nm and λ_{Em} = 415-450 nm), and red to nanogels containing AlexaFluor633-labeled streptavidin (λ_{Ex}= 638 nm and λ_{Em} = 645-700 nm).

Transfection of enzyme-loaded lipoproplexes

We finally investigated whether the lipoproplexes could be used as carriers for an active enzyme, and if the enzyme would keep its catalytic activity after transfection inside the cells. For this purpose, bt-DNA was directly crosslinked in one step with streptavidin conjugated to alkaline phosphatase (ALP) enzyme (Figure 4A) (26) to give functionalized nanogels (ALP-NGs). The formation of ALP-NGs was characterized by AFM imaging (Figures S8) and the concentration of streptavidin-ALP conjugate of 15 nM (for 1 µM of bt-DNA in phosphate groups) was selected for further experiments, giving an apparent diameter of 133 ± 41 nm (Figure S1D). This ratio of streptavidin-ALP to bt-DNA corresponds to up to 100 enzymes per nanogel. The complexation of non-fluorescent ALP-NGs with FITC-labeled liposomes was then confirmed by flow cytometry (Figure S9). We observed that complexation with functionalized nanogels led to increase of mean fluorescence signal distribution of liposomes from the charge ratio R+/- = 0.75 (i.e. 0.5 µM liposomes for 2 µM bt-DNA). Such a low R+/- was thus sufficient for the formation of ALP-loaded lipoproplexes (ALP-LPX).

We then checked if ALP enzyme kept its catalytic activity within the lipoproplexes *in vitro*. For the assay, 9H-(1,3-dichloro-9,9-dimethylacridin-2-one-7-yl) phosphate, diammonium salt (DDAO-P) fluorogenic substrate was used to follow the hydrolysis of its phosphate moieties by alkaline phosphatase via appearance of far-red fluorescence emission of the resulting DDAO. We found that incorporation of the ALP into the nanogels only slightly decreased the catalytic activity of the enzyme to 88% (Figure S10). Adding liposomes to the ALP alone did not affect its activity, whereas within ALP-loaded lipoproplexes the enzyme conserved 79% of its initial catalytic activity, as compared to the activity of the native ALP-streptavidin conjugate. The ALP enzyme thus stayed available to the DDAO-P substrate and catalytically active even after loading into the DNA nanogels and their complexation with cationic lipids.

Finally, transfection of ALP-functionalized lipoproplexes (ALP-LPX) into B16 cells was investigated (Figure 4B). The cells were treated with ALP-LPX and washed to remove any non-transfected nanogels. DDAO-P substrate was then added into the cell medium, and after 1 hour of incubation the cells were rinsed again and intracellular fluorescence of the hydrolyzed DDAO was analyzed by flow cytometry (Figure 4C) and fluorescence microscopy (Figure 4D,E, S11 and S12). We found that even in absence of added ALP, the B16 cells were able to slightly hydrolyze the DDAO-P substrate giving a basal level of alkaline phosphatase activity (35). Flow cytometry showed no effect of adding enzyme alone and enzyme in presence of liposomes on the fluorescence of the cells. The distribution of fluorescence of hydrolyzed substrate slightly increased when cells were incubated with ALP-functionalized nanogels (ALP-NG) without liposomes, but the increase in fluorescence was much stronger when the cells were transfected with ALP-LPX (Figure 4E). We repeated this experiment in triplicates, and analyzed the transfection efficiency by fluorescence microscopy. Figure S12 shows fluorescence distributions for 3 individual experiments, and Figure 4D gives the average fluorescence value of the triplicated transfection experiments normalized by the basal level of ALP activity inside the B16 cells treated with phosphate buffer only. We systematically observed that fluorescence intensity corresponding to the hydrolyzed substrate inside the cells transfected with ALP-LPX, was higher than for the controls containing phosphate buffer only, free enzyme (free ALP), ALP with liposomes or ALP-functionalized nanogels without liposomes. In additional control we compared ALP enzymatic activity inside cells transfected with functionalized and non-functionalized LPX. Figure S13 demonstrates that no enhancement of ALP enzymatic activity after transfection of the enzyme-free LPX was observed, indicating that the increased enzymatic activity in ALP-LPX was due to the catalytic activity of transfected enzyme, and not a result of increasing the basal expression of alkaline phosphatase due to the interaction of lipoproplexes with cellular environment. All these results show that the ALP has been efficiently transfected inside the cells in its active state via functionalized lipoproplexes. To our knowledge, it is a first example of efficient transfection of a large local number of active enzyme molecules embedded into DNA nanogels (up to 100 enzyme molecules per nanogel particle).

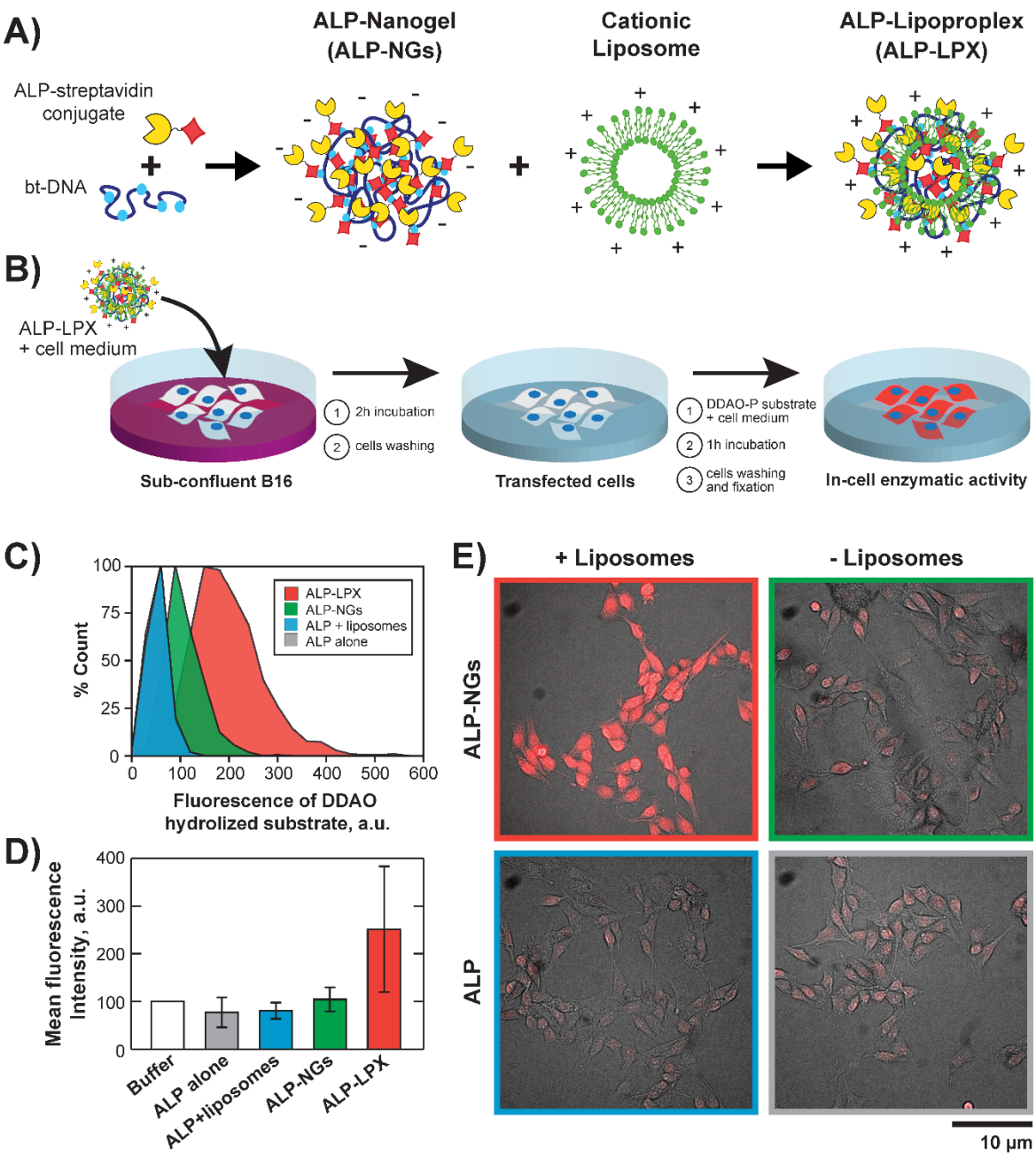

Figure 4. Transfection of ALP-functionalized lipoproplexes and enzymatic activity assay inside the cells. A) Preparation of ALP-loaded lipoproplexes (ALP-LPX), B) Schematic representation of the experimental procedure for transfection and measurement of ALP activity inside the cells. C) Flow cytometry distribution of hydrolyzed DDAO substrate inside transfected B16 cells with APL-LPX and in control samples. The distribution for ALP alone control is not visible, as it has practically the same shape as the one for ALP+liposomes control. D) Mean ± sd for normalized fluorescence intensities of hydrolyzed DDAO. White bar shows intrinsic ALP activity (normalized to 100 %) for cells incubated with the phosphate buffer (in absence of ALP). E) Example of combined transmission and fluorescence microscopy images of hydrolyzed DDAO substrate after treatment of B16 cells with enzyme alone (ALP) or enzyme loaded into DNA nanogels (ALP-NGs) in presence and in absence of liposomes.

Discussion

We reported a new vector-carrier-cargo platform called lipoproplex, schematically represented in the Figure S14, and demonstrated its ability to transport active proteins through the cell membrane. For this purpose, we used DNA

nanogels cross-linked via streptavidin-biotin interactions. This platform enables loading of the protein cargo into DNA carrier in two ways (i.e. using either streptavidinated or biotinylated cargo proteins) thus opening the possibility of large number of functionalities that can be potentially introduced into a single nanogel. We used cationic liposomes for the vectorization of DNA-protein NGs and renamed the resulting complex as "lipoproplex", which evokes the complex between DNA and liposomes (i.e. lipoplex) but is intended to emphasize the importance of the protein component in our DNA-protein nanogels. Three-dimensional structure of the nanogels demands lower concentration of cationic liposomes for efficient transfection (down to R+/- = 0.75), which in combination with intrinsic biocompatibility of DNA nanoscaffold results in non-toxic protein transfection system as demonstrated by the MTT assay. For a proof of concept, here we investigated transfection of two proteins: biotinylated fluorescent protein GFP and the enzyme alkaline phosphatase conjugated to streptavidin. In both cases, the complexation with cationic liposomes and subsequent transfection did not affect the respective properties of the proteins: GFP retained its fluorescence emission whereas the ALP kept its efficiency to hydrolyze the DDAO-P substrate. Both strategies thus proved to be adapted for the nanogels functionalization.

By considering that all streptavidin-ALP conjugates enter the nanogels and each NG consists of 1 DNA scaffold, in our conditions (15 nM of strep-ALP for 1 µM of bt-DNA in phosphates) each nanogel can contain up to 100 loaded enzyme molecules. By assuming the nanogels to have spherical morphology and 130 nm diameter, the local concentration of the loaded protein can be evaluated to around 130 µM. High number of potentially loadable proteins can be useful for transfection of multifunctional nanogels containing a large number of different proteins, and the high local concentration of the loaded proteins is promising for biomedical applications. This approach can thus be of particular interest for co-transfection of several active enzymes at controlled stoichiometry. Co-transfection of genes coding for different enzymes was suggested for cancer therapy (36, 37) and treatment of metabolic diseases (38). But it was shown in some cases to result in the expression of only one or the other enzyme rather than the desired dual expression of both enzymes, (39) because of the competition for the use of intracellular resources available for gene expression. (40) Direct transfection of NGs containing defined enzymatic composition avoids the co-expression step and can thus overcome this issue. Moreover, high local enzyme concentrations within the nanogels can be of particular interest for creating or restoring complex metabolic pathways requiring close spatial positioning of several catalytic processes within an enzymatic cascade.

Conclusions

In conclusion, we presented a new DNA-protein nanogel platform for the transport of active loaded proteins into living cells. The loaded proteins have been efficiently internalized by the cells while keeping their specific properties, which underlines potential therapeutic interest of lipoproplexes for transfection and co-transfection of active enzymes. We anticipate that DNA-protein nanogels could be employed as nanoscaffold for the transport of other biological and chemical entities, not only by incorporating them into the nanogel by streptavidin-biotin binding, but also by orthogonal binding into DNA double helix (i.e. intercalative drugs, such as doxorubicin). (24) Moreover, the commercial availability of biotinylated or streptavidinated recombinant proteins, nanoparticles,

aptameric sequences or antibodies for the specific recognition of target molecules, opens up the possibility of using nanogels as universal scaffolds with a high degree of functionalizability that not only could encapsulate a number of desired features in a single nanosized material, but also could protect the incorporated entities from biological microenvironment. All these results underline great potential of using DNA transfection agents for functionalizable soft DNA nanomaterials.

The authors declare no competing interest.

References

1. C. D. Kusmierz, K. E. Bujold, C. E. Callmann, C. A. Mirkin, Defining the Design Parameters for in Vivo Enzyme Delivery Through Protein Spherical Nucleic Acids. *ACS Cent. Sci.* **6**, 815–822 (2020).
2. D. Samanta, S. B. Ebrahimi, C. D. Kusmierz, H. F. Cheng, C. A. Mirkin, Protein Spherical Nucleic Acids for Live-Cell Chemical Analysis. *J. Am. Chem. Soc.* **142**, 13350–13355 (2020).
3. J. R. Kintzing, M. V. Filsinger Interrante, J. R. Cochran, Emerging Strategies for Developing Next-Generation Protein Therapeutics for Cancer Treatment. *Trends Pharmacol. Sci.* **37**, 993–1008 (2016).
4. D. S. Dimitrov, "Therapeutic Proteins" in *Physiology & Behavior*, (2012), pp. 1–26.
5. S. N. Dean, K. B. Turner, I. L. Medintz, S. A. Walper, Targeting and delivery of therapeutic enzymes. *Ther. Deliv.* **8**, 577–595 (2017).
6. V. Maximov, V. Reukov, A. A. Vertegel, Targeted delivery of therapeutic enzymes. *J. Drug Deliv. Sci. Technol.* **19**, 311–320 (2009).
7. R. J. Desnick, E. H. Schuchman, Enzyme Replacement Therapy for Lysosomal Diseases: Lessons from 20 Years of Experience and Remaining Challenges. *Annu. Rev. Genomics Hum. Genet.* **13**, 307–335 (2012).
8. D. Concolino, F. Deodato, R. Parini, Enzyme replacement therapy: efficacy and limitations. *Ital. J. Pediatr.* **44**, 120 (2018).
9. M.-F. Penet, Z. Chen, C. Li, P. T. Winnard, Z. M. Bhujwalla, Prodrug enzymes and their applications in image-guided therapy of cancer: tracking prodrug enzymes to minimize collateral damage. *Drug Deliv. Transl. Res.* **2**, 22–30 (2012).
10. V. K. Yata, S. Banerjee, S. S. Ghosh, Folic Acid Conjugated-Bio Polymeric Nanocarriers: Synthesis, Characterization and In Vitro Delivery of Prodrug Converting Enzyme. *Adv. Sci. Eng. Med.* **6**, 388–392 (2014).
11. V. Raman, *et al.*, Intracellular delivery of protein drugs with an autonomously lysing bacterial system reduces tumor growth and metastases. *Nat. Commun.* **12**, 6116 (2021).
12. Y. Tian, M. V. Tirrell, J. L. LaBelle, Harnessing the Therapeutic Potential of Biomacromolecules through Intracellular Delivery of Nucleic Acids, Peptides, and Proteins. *Adv. Healthc. Mater.* **11**, 2102600 (2022).
13. R. Goswami, T. Jeon, H. Nagaraj, S. Zhai, V. M. Rotello, Accessing Intracellular Targets through Nanocarrier-Mediated Cytosolic Protein Delivery. *Trends Pharmacol. Sci.* **41**, 743–754 (2020).
14. S. Miersch, S. S. Sidhu, Intracellular targeting with engineered proteins. *F1000Research* **5**, 1947 (2016).

15. A. Fu, R. Tang, J. Hardie, M. E. Farkas, V. M. Rotello, Promises and Pitfalls of Intracellular Delivery of Proteins. *Bioconjug. Chem.* **25**, 1602–1608 (2014).

16. D. S. Pisal, M. P. Kosloski, S. V. Balu-Iyer, Delivery of Therapeutic Proteins. *J. Pharm. Sci.* **99**, 2557–2575 (2010).

17. M. Oba, M. Tanaka, Intracellular Internalization Mechanism of Protein Transfection Reagents. *Biol. Pharm. Bull.* **35**, 1064–1068 (2012).

18. A. Dhankher, W. Lv, W. T. Studstill, J. A. Champion, Coiled coil exposure and histidine tags drive function of an intracellular protein drug carrier. *J. Control. Release* **339**, 248–258 (2021).

19. Y. Li, J. A. Champion, Self-assembling nanocarriers from engineered proteins: Design, functionalization, and application for drug delivery. *Adv. Drug Deliv. Rev.* **189**, 114462 (2022).

20. L. He, J. Mu, O. Gang, X. Chen, Rationally Programming Nanomaterials with DNA for Biomedical Applications. *Adv. Sci.* **8**, 2003775 (2021).

21. M. C. P. Mendonça, A. Kont, P. S. Kowalski, C. M. O'Driscoll, Design of lipid-based nanoparticles for delivery of therapeutic nucleic acids. *Drug Discov. Today* **28**, 103505 (2023).

22. J. D. Brodin, A. J. Sprangers, J. R. McMillan, C. A. Mirkin, DNA-Mediated Cellular Delivery of Functional Enzymes. *J. Am. Chem. Soc.* **137**, 14838–14841 (2015).

23. A. Ora, *et al.*, Cellular delivery of enzyme-loaded DNA origami. *Chem. Commun.* **52**, 14161–14164 (2016).

24. Y. Ryu, *et al.*, Modular protein–DNA hybrid nanostructures as a drug delivery platform. *Nanoscale* **12**, 4975–4981 (2020).

25. L. Zhou, M. Morel, S. Rudiuk, D. Baigl, Intramolecularly Protein-Crosslinked DNA Gels: New Biohybrid Nanomaterials with Controllable Size and Catalytic Activity. *Small* **13**, 1700706 (2017).

26. M. Mariconti, M. Morel, D. Baigl, S. Rudiuk, Enzymatically Active DNA-Protein Nanogels with Tunable Cross-Linking Density. *Biomacromolecules* **22**, 3431–3439.

27. S. A. Bowden, B. L. Foster, "Alkaline Phosphatase Replacement Therapy for Hypophosphatasia in Development and Practice" in *Advances in Experimental Medicine and Biology*, (2019), pp. 279–322.

28. G. Byk, D. Scherman, B. Schwartz, C. Dubertret, Lipopolyamines as transfection agents and pharmaceutical uses thereof. *US Pat. 6171612* (2001).

29. D. C. Arruda, *et al.*, Spheroplexes: Hybrid PLGA-cationic lipid nanoparticles, for in vitro and oral delivery of siRNA. *J. Control. Release* **350**, 228–243 (2022).

30. J. Li, *et al.*, Self-Assembled Multivalent DNA Nanostructures for Noninvasive Intracellular Delivery of Immunostimulatory CpG Oligonucleotides. *ACS Nano* **5**, 8783–8789 (2011).

31. L. Liang, *et al.*, Single-Particle Tracking and Modulation of Cell Entry Pathways of a Tetrahedral DNA Nanostructure in Live Cells. *Angew. Chemie Int. Ed.* **53**, 7745–7750 (2014).

32. A. S. Walsh, H. Yin, C. M. Erben, M. J. A. Wood, A. J. Turberfield, DNA Cage Delivery to Mammalian Cells. *ACS Nano* **5**, 5427–5432 (2011).

33. S. Wang, H. Guo, Y. Li, X. Li, Penetration of nanoparticles across a lipid bilayer: effects of particle stiffness

and surface hydrophobicity. *Nanoscale* **11**, 4025–4034 (2019).

34. T. Mosmann, Rapid colorimetric assay for cellular growth and survival: Application to proliferation and cytotoxicity assays. *J. Immunol. Methods* **65**, 55–63 (1983).

35. S. Burghoff, *et al.*, Growth and metastasis of B16-F10 melanoma cells is not critically dependent on host CD73 expression in mice. *BMC Cancer* **14**, 898 (2014).

36. Y. Liu, *et al.*, Enhancement of immunogenicity of tumor cells by cotransfection with genes encoding antisense insulin-like growth factor-1 and B7.1 molecules. *Cancer Gene Ther.* **7**, 456–465 (2000).

37. W. Uckert, *et al.*, Double Suicide Gene (Cytosine Deaminase and Herpes Simplex Virus Thymidine Kinase) but Not Single Gene Transfer Allows Reliable Elimination of Tumor Cells In Vivo. *Hum. Gene Ther.* **9**, 855–865 (1998).

38. G. De Sabbata, *et al.*, Long-term correction of ornithine transcarbamylase deficiency in Spf-Ash mice with a translationally optimized AAV vector. *Mol. Ther. - Methods Clin. Dev.* **20**, 169–180 (2021).

39. S. Gupta, *et al.*, Engineering protein glycosylation in CHO cells to be highly similar to murine host cells. *Front. Bioeng. Biotechnol.* **11**, 1–14 (2023).

40. R. Di Blasi, M. M. Marbiah, V. Siciliano, K. Polizzi, F. Ceroni, A call for caution in analysing mammalian co-transfection experiments and implications of resource competition in data misinterpretation. *Nat. Commun.* **12**, 2545 (2021).

Acknowledgment

This work was supported by Agence Nationale de la Recherche (ANR) grants ANR-18-CE07-0001 (S.R.) and ANR-18-CE06-0019 (D. B.). We thank the Plateforme d'Imagerie Cellulaire et Moléculaire, US25 Inserm, UAR3612 CNRS, Université Paris Cité, Faculté de Pharmacie, Paris, France for access to confocal microscopy.